Available at www.sciencedirect.com

ScienceDirect

journal homepage: www.elsevier.com/locate/he

# Turbulent burning velocity of hydrogen–air premixed propagating flames at elevated pressures

*Toshiaki Kitagawa*, Takashi Nakahara, Kosuke Maruyama, Kunihiro Kado, Akihiro Hayakawa, Shoichi Kobayashi*

*Department of Mechanical Engineering, Faculty of Engineering, Kyushu University, 744 Motooka, Nishi-ku, Fukuoka 819-0395, Japan*

ARTICLE INFO

*Article history:*
Received 16 April 2008
Received in revised form
12 June 2008
Accepted 12 June 2008
Available online 10 September 2008

*Keywords:*
Hydrogen
Combustion
Premixed turbulent flame
Burning velocity
Effect of pressure
Lewis number
Markstein number

ABSTRACT

Lewis number represents the thermo-diffusive effects on laminar flames. That of hydrogen–air mixture varies extensively with the equivalence ratio due to the high molecular diffusivity of hydrogen. In this study, the influences of pressure and thermo-diffusive effects on spherically propagating premixed hydrogen–air turbulent flames were studied using a constant volume fan-stirred combustion vessel. It was noted that the ratio of the turbulent to unstretched laminar burning velocity increased with decreasing equivalence ratio and increasing mixture pressure. Turbulent burning velocity was dominated by three factors: (1) purely hydrodynamic factor, turbulence Reynolds number, (2) relative turbulence intensity to reaction speed, the ratio of turbulence intensity to unstretched laminar burning velocity, and (3) sensitivity of the flame to the stretch due to the thermo-diffusive effects, Lewis and Markstein numbers. A turbulent burning velocity correlation in terms of Reynolds and Lewis numbers is presented.



## 1. Introduction

Hydrogen is an alternative fuel for internal combustion engines because of its less emissions properties of unburned hydrocarbon, carbon monoxide, carbon dioxide, and particulates [1]. Lean mixture operation is possible because hydrogen has a wider flammable range and larger burning velocity than other common fuels. It can yield a higher thermal efficiency of hydrogen engines due to the reduction of the pumping loss. Emission levels of $NO_x$ may be also reduced by lean combustion [1,2].

At the same time, however, characteristic features of hydrogen also tend to cause some problems such as preignition [1,2], the onset of knock [2,3]. In order to overcome these problems, it is important to understand the properties of hydrogen flame.

In addition to hydrogen, various types of fuel containing hydrogen have been also investigated in order to improve the performance of engines [4], to use biomass as fuel [5], or to increase the safety of hydrogen by hydrocarbon substitution [6]. A small amount of hydrogen addition introduced changes in the flame characteristics [4]. Thus, this study investigated the fundamental aspects of hydrogen flames from the following viewpoints.

Internal combustion engines are operated at elevated pressures. However, only a few fundamental studies on combustion of hydrogen and hydrocarbons have been carried out at elevated pressures [7–14]. To date, these studies have

* *Corresponding author*. Tel.: +81 92 802 3148; fax: +81 92 802 0001.
E-mail address: toshi@mech.kyushu-u.ac.jp (T. Kitagawa).

0360-3199/$ – see front matter © 2008 International Association for Hydrogen Energy. Published by Elsevier Ltd. All rights reserved.
doi:10.1016/j.ijhydene.2008.06.013

indicated that flames at elevated pressures have rather different behaviour [8–14] to the corresponding flames observed at atmospheric pressure.

Studies of burning velocity at elevated pressure such as those by Bradley et al. [8], Gu et al. [9], and Faeth et al. [10,11] have reported that consideration of the influence of flame stretch via aerodynamic strain and/or the flame curvature on laminar flames is important to establish reliable laminar burning velocity measurements. The response of the laminar burning velocity of a flame to stretch has been characterised by a Markstein number [15], which has proven to be sensitive to mixture strength and pressure [8–11,14,16,17].

Bradley et al. [18] and Law et al. [13] have reported the transition to cellular flame structures at smaller flame radii for higher pressures for outwardly propagating spherical flames. Hence, the flame instability proved to be influenced by increasing mixture pressure. Experimental observations of laminar and turbulent combustion using burner-stabilized flames by Kobayashi et al. [12,19,20] showed that local flame structures were finer and more convoluted at elevated pressures.

Turbulent burning velocities have also been investigated at elevated pressures [14,21,22]. Increased turbulent burning velocities (relative to the unstretched laminar burning velocity) were reported for those mixtures most sensitive to flame instability. Hence, turbulence may well influence local flame stretch and affect the burning velocity with increasing mixture pressure.

In this study, the laminar and turbulent burning velocities were investigated for outwardly propagating hydrogen–air flames in an optically accessed combustion vessel, for initial pressures in the range of 0.10–0.50 MPa. The Lewis number of hydrogen–air mixture varies widely with the equivalence ratio compared to common hydrocarbons in laboratories such as methane and propane. Lean flames with small Lewis numbers were observed quite unstable. Unstretched laminar burning velocities and Markstein numbers could not be determined from those explosions carried out at laminar conditions. They were obtained by the numerical simulation using detailed reaction-kinetic mechanism.

The influences of the turbulence intensity, mixture pressure, and Markstein number on turbulent flame propagation were investigated. A turbulent burning velocity correlation for application to elevated pressures is proposed in terms of the Reynolds and Lewis numbers and ratio of turbulence intensity to unstretched laminar burning velocity.

## 2. Experimental apparatus and procedures

Experiments were carried out using the constant volume bomb apparatus outlined schematically in Fig. 1. The combustion vessel is comprised of three 265 mm diameter cylinders, which intersect orthogonally. The total volume of the chamber is approximately 35,000 $cm^3$ or equivalent to that of a sphere with a diameter of 40.6 cm. The vessel has been designed to withstand the maximum pressure of 10 MPa expected for explosions carried out with an initial pressure of up to 1.0 MPa.

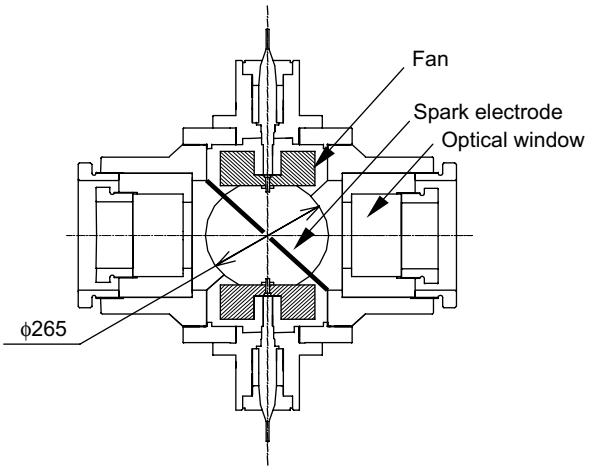


**Fig. 1 – Schematic figure of combustion chamber.**

Combustible hydrogen–air mixture quantities were prepared in the vessel according to the required partial pressures of hydrogen and air. In the present study, the equivalence ratio, $\varphi$ was 0.4, 0.6, 0.8, and 1.0. Explosions were carried out with initial mixture pressures, $P_i$ of 0.10, 0.25, and 0.50 MPa. The initial temperature of the mixture was kept 300 K for all experiments.

The two fans (mounted at the top and bottom of the vessel and driven by electric motors) were operated after mixture preparation to ensure proper mixing. In the laminar combustion experiments, mixture was ignited 1 min after the two fans were stopped and mixture flow in the vessel decayed completely.

In the turbulent combustion experiments, the fans were operated during explosions. Relationships between the fan shaft rotational speed, turbulence intensity, $u'$, and longitudinal integral length scale, $L_f$ have been conducted previously using Particle Image Velocimetry (PIV). Turbulence intensities of 0.80 and 1.59 m/s were adopted. The integral length scale proved to be 10.3 mm and was independent of all examined initial pressures and rotational fan speeds.

Mixture was ignited by the electric spark at the center of the chamber. The spark electrodes had a diameter of 1.8 mm and the spark gap was set to 3 mm, the spark energy was 1.4 J. Flame propagation was observed using schlieren photography via two 160 mm diameter windows mounted oppositely. Explosions were recorded using a Phantom v4.1 high-speed digital camera operated at 1000–25000 f/s with $512 \times 512$–$256 \times 32$ pixel image resolution, respectively.

Laminar and turbulent burning velocities have been obtained from flame radius [8,14,21,22]. With an initial pressure of 0.10 MPa, the maximum pressure rise in which the entire flame front is visible (flame radius of less than 80 mm) is 0.05 MPa. Hence, measurements were considered to have been completed at the adopted approximate initial pressure and temperature.

At least three explosions were carried out at each condition. Experimental scatter of measured burning velocities was within a range of 5–10% of average value at most conditions, and it exceeded 15% at some conditions. As shown in the

following sections, however, the scatter at each condition was small enough to distinguish the variations of the data by the differences of the conditions such as the equivalence ratio, mixture pressure and turbulence intensity.

## 3. Laminar burning velocity

Previous studies of spherically propagating laminar flames showed the burning velocity to be influenced by the flame stretch rate [8–11]. Hence, unstretched laminar burning velocities were obtained using the following approach.

The observed flame radius, $r$ was adopted to determine a stretched laminar burning velocity, $u_n$ during flame propagation [8,9].

$$u_n = \frac{\rho_b}{\rho_u} S_n = \frac{\rho_b}{\rho_u} \frac{dr}{dt} \quad (1)$$

Where, $\rho_u$ and $\rho_b$ are the densities of the unburned mixture and burned gas respectively. $S_n$ is the flame propagation speed and $t$ is time.

The flame stretch rate, $\alpha$ imposed on the spherically propagating flame was calculated using the flame front area, $A$ or the flame radius, $r$ according to Eq. (2) [8,9,23–25].

$$\alpha = \frac{1}{A}\frac{dA}{dt} = \frac{2}{r} S_n = \frac{2}{r}\frac{dr}{dt} \quad (2)$$

The difference between the stretched, $u_n$ and the unstretched laminar burning velocity, $u_l$ was considered proportional to the stretch rate [25–29] and the Markstein length, $L$ [15]. The Markstein length was determined by Eq. (3) to the relationship between $\alpha$ and $u_n$ [8,9].

$$u_l - u_n = L\alpha \quad (3)$$

The unstretched laminar burning velocity, $u_l$ was derived as the intercept value of $u_n$ at $\alpha = 0$ by the extrapolation of the stretched laminar burning velocity to an infinite flame radius (or a stretch rate of zero) [8,9].

Eq. (3) can be non-dimensionalised by dividing by the unstretched laminar burning velocity and the laminar flame thickness, $\delta_l$:

$$\frac{u_l - u_n}{u_l} = KMa \quad (4)$$

in which $K$ ($= \alpha\delta_l/u_l$) is the flame stretch rate and $Ma$ ($= L/\delta_l$) is the Markstein number [8,9].

Laminar explosions carried out for $\varphi = 1.0$ at $P_i = 0.06$, 0.10, and 0.25 MPa are presented in Fig. 2 in terms of stretch rate, $\alpha$ versus laminar burning velocity, $u_n$. Stretch rate, $\alpha$ decreased during flame propagation. Open circles denote the experimental results. It was noted that increased stretch rates resulted in reduced stretched laminar burning velocity at $P_i = 0.06$ MPa. There seemed linear relationship between $\alpha$ and $u_n$ applicable to Eq. (3). This relationship was characterised by a positive Markstein length.

The observed rapid increase in the recorded laminar burning velocity for reducing stretch rates was noted at $P_i = 0.10$ MPa. It was proved consistent with the visual formation of cells and cracks on the flame surface due to the flame instability [8]. Since the local stretch rates and surface areas are unknown, this regime is not applicable in the analysis.

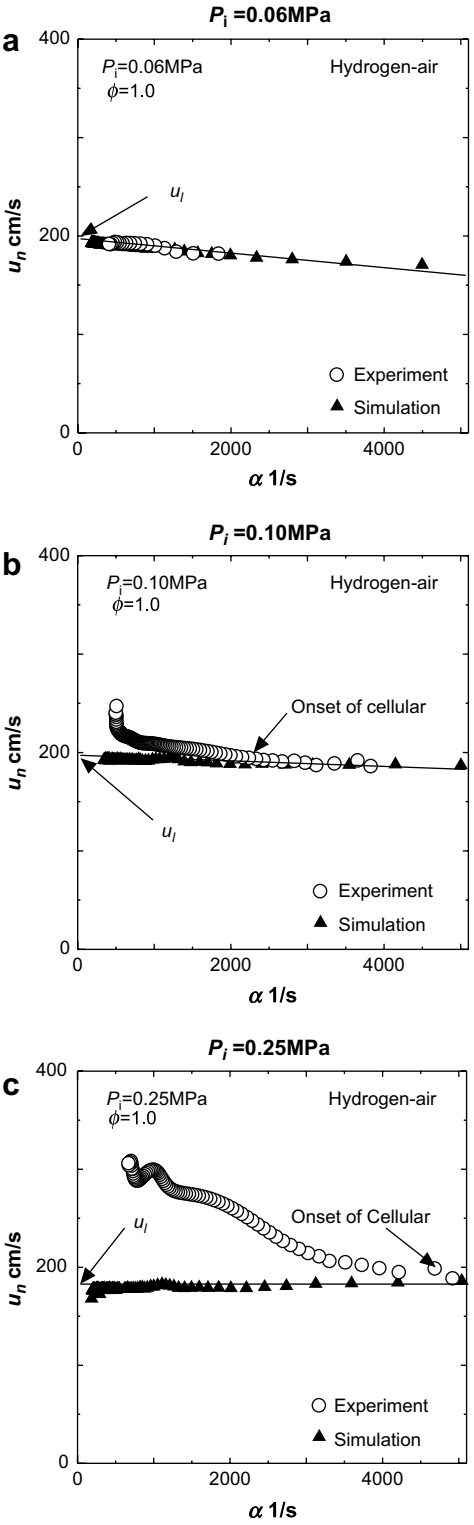


**Fig. 2 – Laminar burning velocity of hydrogen–air mixture, $u_n$ versus stretch rate, $\alpha$ of explosions at equivalence ratios, $\varphi$ of 1.0 with initial pressure, $P_i$ of 0.06, 0.10, and 0.25 MPa.**

The flames became cellular soon after ignition at initial mixture pressures, $P_i = 0.25$ and 0.50 MPa. The regime of flame stretch rate was too narrow to apply Eq. (3) for reliable analysis.

Thus the numerical simulation of outwardly propagating flames were carried out by COSILAB [30] using a detailed chemical-kinetic mechanism by Curran et al. [31]. Any disturbances triggering cell formation do not exist in the numerical simulation. Solid triangles denote the simulation results. The results were compared with those of experiments. Simulation results corresponded closely with ones by experiments at initial mixture pressures, $P_i$ of 0.06 where flames did not show the flame instability in the experiments. At $P_i = 0.10$ MPa, they also show good agreements with experiments until the onset of cellular flame. Hence, the numerical simulation was considered reliable at all initial mixture pressures including 0.25 and 0.50 MPa.

The unstretched laminar burning velocity, $u_l$ and the Markstein number, *Ma* for hydrogen–air mixtures at $\varphi = 0.4$, 0.6, 0.8, and 1.0 are shown in Fig. 3a, b. The unstretched laminar burning velocity, $u_l$ decreased as the initial pressure, $P_i$ increased.

Pressure index, $n$ was defined by Eq. (5).

$$\frac{u_l}{u_{l0}} = \left(\frac{P}{P_0}\right)^n \tag{5}$$

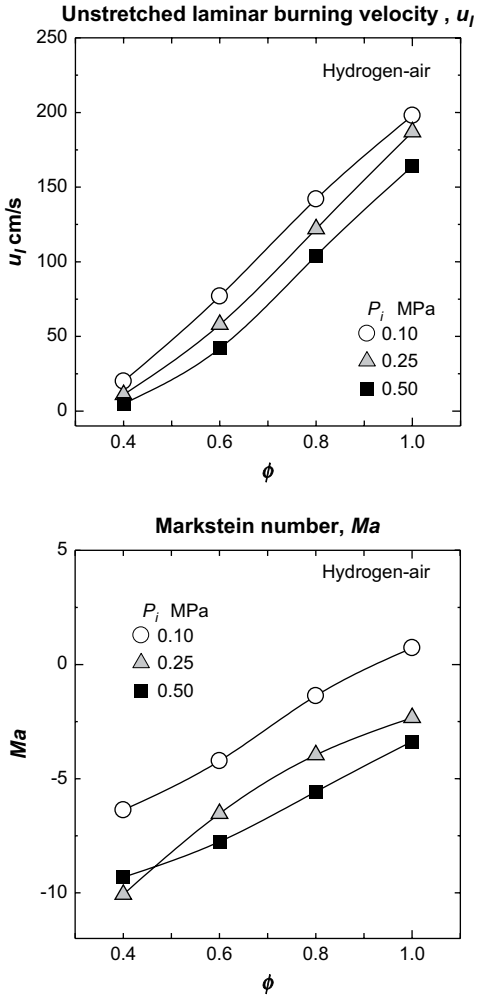


**Fig. 3 – Unstretched laminar burning velocity of hydrogen–air mixture, $u_l$ and Markstein number, *Ma* obtained by numerical simulation at the adopted initial pressures, $P_i$ and equivalence ratios, $\varphi$.**

Here, $P_0$ is 0.10 MPa and $u_{l0}$ is $u_l$ at 0.10 MPa. Pressure index, $n$ increased with increasing equivalence ratio and was −0.748, −0.331, −0.173, and −0.088 at $\varphi = 0.4$, 0.6, 0.8, and 1.0, respectively.

The Markstein number, *Ma* increased as the equivalence ratio, $\varphi$ increased for all of the examined initial pressures. The Markstein number decreased at all equivalence ratios for increasing mixture pressures, except for $\varphi = 0.4$.

## 4. Turbulent burning velocity

Turbulent burning velocity, $u_{tn}$ during the turbulent flame propagation was determined from measurements by adopting Eq. (6).

$$u_{tn} = \frac{\rho_b}{\rho_u}\frac{dr}{dt} \tag{6}$$

where $r$ is the mean flame radius, derived by calculating a circle of which has equivalent area to the turbulent flame observed experimentally [21]. This flame radius had a linear correlation with the radius, which was defined in the tomography image such that the volume of unburned mixture inside this radius is equal to the volume of burned gas outside it [21].

Examples of turbulent explosions carried out at $\varphi = 0.4$ and 1.0 at 0.10 and 0.50 MPa with a turbulence intensity of 1.59 m/s are presented in Fig. 4 in terms of flame radius versus turbulent burning velocity. Turbulent burning velocities kept increasing and did not show specific constant values within the observation range of the flame radius at any conditions. Fully developed values were not obtained in this study. Thus the turbulent burning velocity at flame radius of 30 mm, $u_{tn(30\ mm)}$ was adopted in the analyses same as Mandilas et al. [14]. However, the adopted approach was more consistent with the development of turbulent burning velocities noted in the combustion chambers of around 50 mm radius of SI engines.

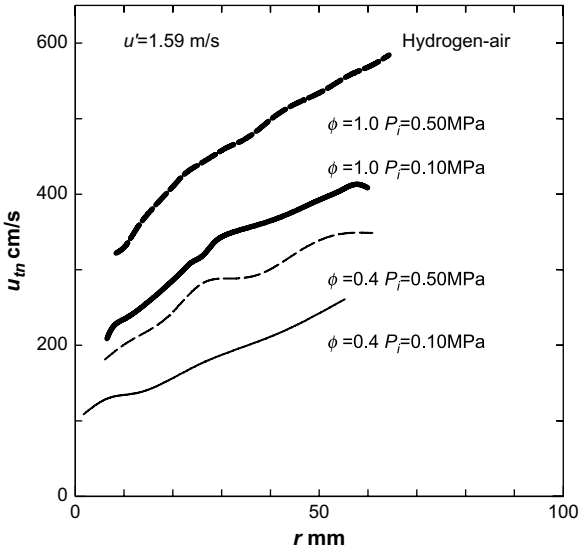


**Fig. 4 – Turbulent burning velocity of hydrogen–air mixture, $u_{tn}$ versus flame radius, $r$ at equivalence ratios, $\varphi$ of 0.4 and 1.0 with initial pressure, $P_i$ of 0.10 and 0.50 MPa.**

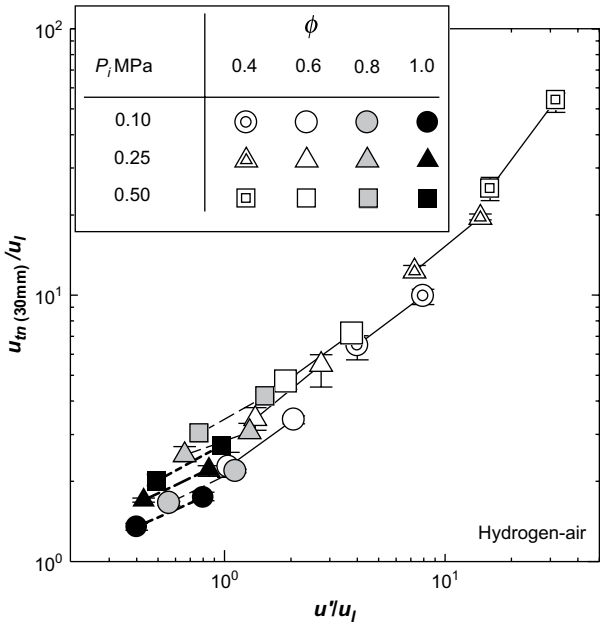


**Fig. 5 – Variation of $u_{tn(30\ mm)}/u_l$ with $u'/u_l$.**

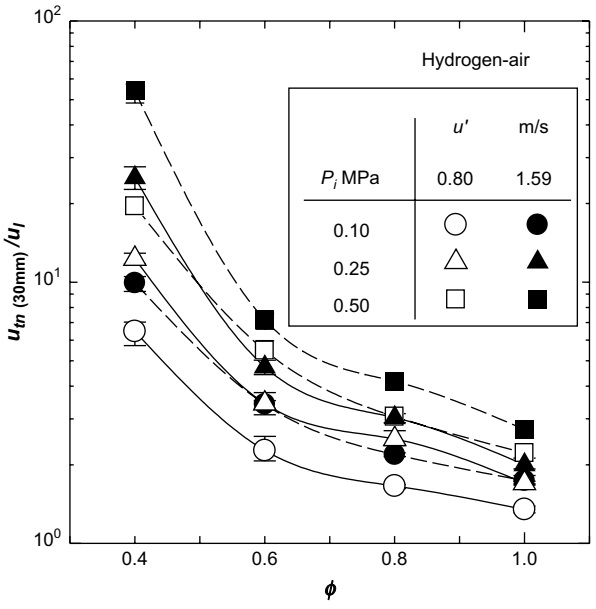


**Fig. 6 – Variation of $u_{tn(30\ mm)}/u_l$ with equivalence ratios, φ.**

## 5. Effects of turbulence intensity, equivalence ratio, and pressure on turbulent burning velocity

The effect of turbulence intensity on turbulent burning velocity at flame radius 30 mm, $u_{tn(30\ mm)}$ is shown in Fig. 5 as the ratio of it to unstretched laminar burning velocity, $u_{tn(30\ mm)}/u_l$. As mentioned in the previous section, experimental scatter was within a range of 10% of average value at most conditions, but it exceeded 15% at some conditions. Experimental scatter range is shown for each condition in the figure. The ratio of turbulent burning velocity to unstretched laminar burning velocity, $u_{tn(30\ mm)}/u_l$ increased as the ratio of turbulence intensity to unstretched laminar burning velocity, $u'/u_l$ increased at all the equivalence ratios and mixture pressures. It is expected that wrinkling of the flame front by turbulence results in a larger flame area and hence larger burning velocity.

Turbulent burning velocity also depended on the equivalence ratio, φ. Fig. 6 shows larger equivalence ratio resulted in decreased $u_{tn(30\ mm)}/u_l$. Thermo-diffusive effects due to the flame stretch induced by the turbulence may affect the turbulent burning velocity because the Markstein number increased with increasing the equivalence ratio as shown in Fig. 3b.

As for the effects of mixture pressure, increased $u_{tn(30\ mm)}/u_l$ were noted with increasing initial pressure as shown in Fig. 7. As the unstretched laminar burning velocity, $u_l$ decreased with mixture pressure, $u'/u_l$ increased with increasing mixture pressure. At the same time, the Markstein number decreased with increasing pressure. Outwardly propagating turbulent flames with a mean overall positive stretch rate would yield increased turbulent burning velocities with increasing pressure. Hence, the local burning velocity with increasing pressure may have been offset by the decreasing Markstein number.

As shown in Fig. 8, $u_{tn(30\ mm)}/u_l$ was larger with smaller Markstein numbers. Turbulence may results in a larger flame front area and large turbulent burning velocity. However, it appears that the adoption of the unstretched laminar burning velocity is insufficient to represent the local burning velocity of the turbulent flame. Turbulent flames are stretched locally

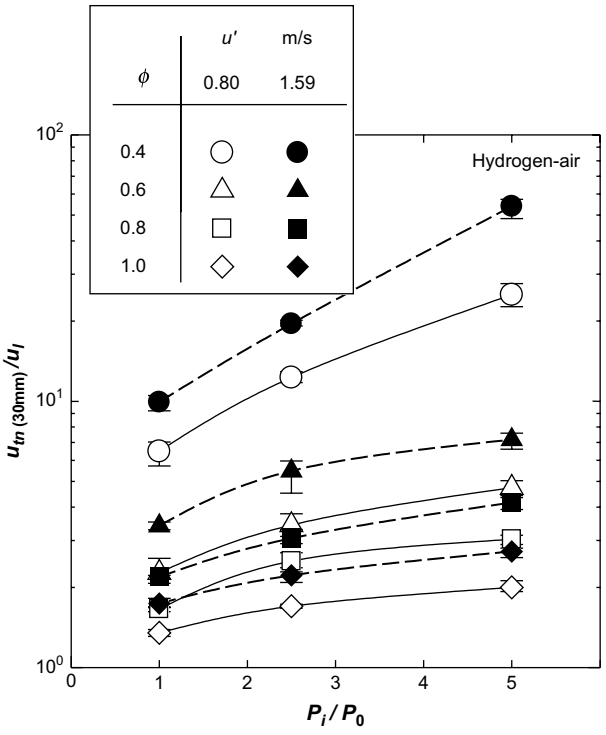


**Fig. 7 – Variation of $u_{tn(30\ mm)}/u_l$ with $P_i/P_0$.**

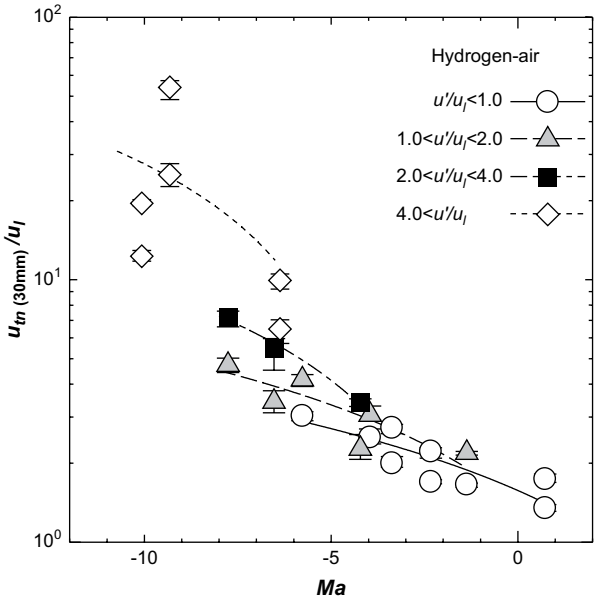


**Fig. 8 – Relationship between $u_{tn(30\ mm)}/u_l$ and Markstein number, *Ma*.**

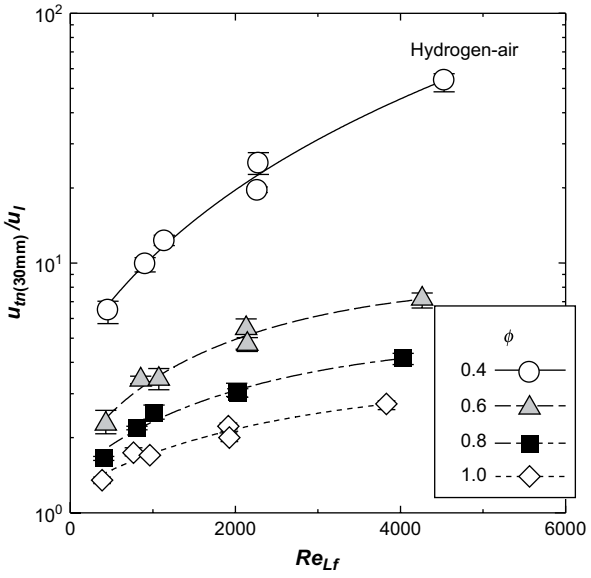


**Fig. 9 – Relationship between $u_{tn(30\ mm)}/u_l$ and turbulence Reynolds number, $Re_{L_f}$.**

and generally in a positive manor [32]. Hence, turbulent flames must have a corresponding local burning velocity, which depending on the Markstein number, may be greater or less than the unstretched laminar burning velocity.

Thus the ratio of turbulence intensity to unstretched laminar burning velocity, $u'/u_l$ and the Markstein number, *Ma* might be dominant factors to the turbulent burning velocity. However, $u_{tn(30\ mm)}/u_l$ seemed to be affected by other factors in addition to $u'/u_l$ and *Ma*, because the values of $u_{tn(30\ mm)}/u_l$ varied within the conditions of almost same $u'/u_l$ and *Ma*.

Increasing pressure also affects aerodynamic aspects of the flame through increasing turbulence Reynolds number. Fig. 9 shows increasing turbulence Reynolds number, $Re_{L_f}$ (= $u'\,L_f/\nu$, $\nu$: kinematic viscosity) based on turbulence intensity, $u'$ and longitudinal integral length scale, $L_f$ resulted in increased $u_{tn(30\ mm)}/u_l$.

Thus the turbulent burning velocity may depend on: (1) purely hydrodynamic factor, turbulence Reynolds number, (2) relative turbulence intensity to reaction speed, the ratio of turbulence intensity to unstretched laminar burning velocity, and (3) sensitivity of the flame to the stretch due to the thermo-diffusive effects, Markstein number.

## 6. A correlation in terms of turbulence Reynolds and Lewis numbers

In practice, Markstein number measurements have proven difficult to obtain without significant experimental or numerical studies, hence turbulent burning velocity correlations have been developed on the basis of *KaLe* (where Lewis number, *Le* is given by the thermal diffusivity divided by the diffusion coefficient of the deficient reactant) such as those proposed by Bradley et al. [33]. Unlike the Markstein number, the Lewis number can be calculated only from mixture properties although these two numbers are both related to the thermo-diffusive effects.

The turbulence Karlovitz number, *Ka* was estimated by Eq. (7).

$$Ka = \frac{\delta_l}{u_l}\Big/\frac{\lambda_g}{u'} \tag{7}$$

Here, $\lambda_g$ is Taylor microscale of turbulence, which was obtained by Eq. (8) [33] with a value of A equal to 16 [34].

$$\frac{\lambda_g^2}{L_f} = A\frac{\nu}{u'} \tag{8}$$

Equation (8) can be modified using the turbulence Reynolds number. Hence,

$$Ka = A^{-0.5}\left(\frac{u'}{u_l}\right)^2 Re_{L_f}^{-0.5} \tag{9}$$

Substitution into the original correlation term of *KaLe* and rearrangement of this leads to

$$\frac{Re_{L_f}}{Le^2} = \left[\frac{A^{-0.5}\left(\frac{u'}{u_l}\right)^2}{KaLe}\right]^2 \tag{10}$$

Thus $Re_{L_f}/Le^2$ may be a practical combined parameter for hydrodynamic turbulence effect and thermo-diffusive effect instead of $Re_{L_f}$ and *Ma*. Three dominant factors of $Re_{L_f}$, $u'/u_l$ and *Ma* shown in the previous section can be reduced into $Re_{L_f}/Le^2$ and $u'/u_l$.

Presented in Fig. 10 are $u_{tn(30\ mm)}/u_l$ obtained at the equivalence ratios of $\varphi = 0.4$, 0.6, and 0.8. All of the data could be grouped into four regimes of $u'/u_l$. In all regimes, $u_{tn(30\ mm)}/u_l$ increased with $Re_{L_f}/Le^2$.

Turbulent combustion may well be influenced by those same aspects which result in the observation of reduced/increased laminar burning velocities with stretch rate in

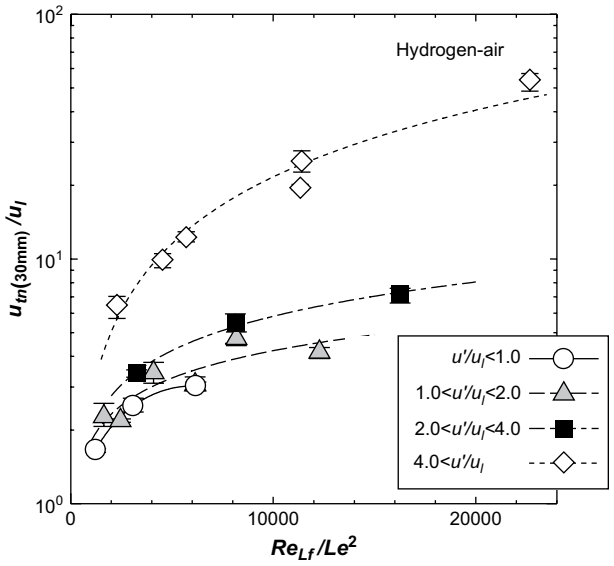


**Fig. 10 – Relationship between $u_{tn(30\ mm)}/u_l$ and $Re_{L_f}/Le^2$.**

laminar flames and characterised by the Markstein number, which is very sensitive to increasing pressure.

Any predictive tool purporting to determine reliable turbulent burning velocities over a range of turbulent intensities and pressures must consider the local turbulent flame structure and those aspects characterised by the Markstein number. Presently, the correlation in terms of Lewis number may well prove reliable enough in practice. Such a correlation could be improved by studying the interaction of local burning velocity within turbulent flames, particularly for flames with very high or low Markstein numbers.

## 7. Conclusions

The effects of pressure on premixed hydrogen–air laminar and turbulent flames were investigated at the equivalence ratios of 0.4, 0.6, 0.8, and 1.0 at the initial pressures of 0.10–0.50 MPa. And outwardly propagating laminar flames were numerically simulated. Unstretched laminar burning velocities and Markstein numbers were obtained. Turbulent burning velocities were obtained with turbulence intensities of 0.80 and 1.59 m/s.

The Markstein number decreased for increasing pressures and for small equivalence ratios. The ratios of turbulent to unstretched laminar burning velocities were shown to increase with increasing pressure and decreasing equivalence ratio. It was noted that turbulent flames were also observed to be influenced by those same aspects characterised by the Markstein number. The effects of turbulence intensity and pressure on the turbulent burning velocity were investigated by the ratio of turbulence intensity to unstretched laminar burning velocity, and turbulence Reynolds number. A turbulent burning velocity correlation in terms of turbulence Reynolds number and Lewis number, similar to that suggested by Bradley et al., was well developed over a range of pressures.

## REFERENCES

[1] Karim GA. Hydrogen as a spark ignition engine fuel. International Journal of Hydrogen Energy 2003;28:569–77.
[2] de Boer PCT, McLean WJ, Homan HS. Performance and emissions of hydrogen fueled internal combustion engines. International Journal of Hydrogen Energy 1976;1:153–72.
[3] Hailin L, Karim GA. Knock in spark ignition hydrogen engines. International Journal of Hydrogen Energy 2004;29:859–65.
[4] Halter F, Chauveau C, Gökalp I. Characterization of the effects of hydrogen addition in premixed methane/air flames. International Journal of Hydrogen Energy 2007;32:2585–92.
[5] Serrano C, Hernández JJ, Mandilas C, Sheppard CGW, Woolley R. Laminar burning behaviour of biomass gasification-derived producer gas. International Journal of Hydrogen Energy 2008;33:851–62.
[6] Law CK, Kwon OC. Effects of hydrocarbon substitution on atmospheric hydrogen–air flame propagation. International Journal of Hydrogen Energy 2004;29:867–79.
[7] Andrews GE, Bradley D. The burning velocity of methane-air mixtures. Combustion and Flame 1972;19:275–88.
[8] Bradley D, Hicks RA, Lawes M, Sheppard CGW, Woolley R. The measurement of laminar burning velocities and Markstein numbers for iso-octane-air and iso-octane-n-heptane-air mixtures at elevated temperatures and pressures in an explosion bomb. Combustion and Flame 1998;115:126–44.
[9] Gu XJ, Haq MZ, Lawes M, Woolley R. laminar burning velocity and Markstein lengths of methane-air mixtures. Combustion and Flame 2000;121:41–58.
[10] Hassan MI, Aung KT, Faeth GM. Measured and predicted properties of laminar premixed methane/air flames at various pressures. Combustion and Flame 1998;115:539–50.
[11] Kwon OC, Faeth GM. Flame/stretch interactions of premixed hydrogen-fueled flames: measurements and predictions. Combustion and Flame 2001;124:590–610.
[12] Qin X, Kobayashi H, Niioka T. Laminar burning velocity of hydrogen–air premixed flames at elevated pressure. Experimental Thermal and Fluid Science 2000;21:58–63.
[13] Tse SD, Zhu DL, Law CK. Morphology and burning rates of expanding spherical flames in $H_2/O_2$/inert mixtures up to 60 atmospheres. Proceedings of the Combustion Institute 2000;28:1793–800.
[14] Mandilas C, Ormsby MP, Sheppard CGW, Woolley R. Effects of hydrogen addition on laminar and turbulent premixed methane and iso-octane-air flames. Proceedings of the Combustion Institute 2007;31:1443–50.
[15] Markstein GH. Experimental and theoretical studies of flame-front stability. Journal of the Aeronautical Sciences 1951:199–216.
[16] Müller UC, Bollig M, Peters N. Approximations for burning velocities and Markstein numbers for lean hydrocarbon and methanol flames. Combustion and Flame 1997;108:349–56.
[17] Sun CJ, Sung CJ, He L, Law CK. Dynamics of weakly stretched flames: quantitative description and extraction of global flame parameters. Combustion and Flame 1999;118:108–28.
[18] Bradley D, Sheppard CGW, Woolley R, Greenhalgh DA, Lockett RD. The development and structure of flame instabilities and cellularity at low Markstein numbers in explosions. Combustion and Flame 2000;122:195–209.
[19] Kobayashi H, Kawabata Y, Maruta K. Experimental study on general correlation of turbulent burning velocity at high pressure. Proceedings of the Combustion Institute 1998;27:941–8.

[20] Kobayashi H, Kawahata T, Seyama K, Fujimari T, Kim JS. Relationship between the smallest scale of flame wrinkles and turbulence characteristics of high-pressure, high-temperature turbulent premixed flames. Proceedings of the Combustion Institute 2002;29:1793–800.
[21] Bradley D, Haq MZ, Hicks RA, Kitagawa T, Lawes M, Sheppard CGW, et al. Turbulent burning velocity, burned gas distribution, and associated flame surface definition. Combustion and Flame 2003;133:415–30.
[22] Lawes M, Ormsby MP, Sheppard CGW, Woolley R. The variation of turbulent burning rate of methane, methanol and iso-octane air mixtures with equivalence ratio at elevated pressure. Combustion Science and Technology 2005;(7).
[23] Law CK. Dynamics of stretched flames. Proceedings of the Combustion Institute 1988;22:1381–402.
[24] Williams FA. Combustion theory: the fundamental theory of chemically reacting flow systems. 2nd ed. Benjamin/Cummings Publishing Company, Inc; 1985.
[25] Matalon M. On flame stretch. Combustion Science and Technology 1983;31:169–81.
[26] Clavin P. Dynamic behavior of premixed flame fronts in laminar and turbulent flows. Progress in Energy and Combustion Science 1985;11:1–59.
[27] Tien JH, Matalon M. On the burning velocity of stretched flame. Combustion Science and Technology 1991;84:238–48.
[28] Davis SG, Quinard J, Searby G. Markstein numbers in counterflow, methane- and propane-air flames: a computational study. Combustion and Flame 2002;130:112–22.
[29] Betchtold JK, Matalon M. The dependence of the Markstein length on stoichiometry. Combustion and Flame 2001;127:1906–13.
[30] COSILAB. The combustion simulation laboratory, version 1.4. Bad Zwischenahn, Germany: Rotexo GmbH & Co. KG, www.SoftPredict.com; 2006. Available from:.
[31] O'Connaire M, Curran HJ, Simmie JM, Pitz WJ, Westbrook CK. A comprehensive modeling study of hydrogen oxidation. International Journal of Chemical Kinetics 2004;36:603–22.
[32] Renou B, Boukhalfa A, Puechberty D, Trinite M. Local scalar flame properties of freely propagating premixed turbulent flames at various Lewis numbers. Combustion and Flame 2000;123:507–21.
[33] Bradley D, Lau AKC, Laws M. Flame stretch rate as a determinant of turbulent burning velocity. Philosophical Transactions of the Royal Society A 1992;338:359–87.
[34] Scott, M.J., Distributions of strain rate and temperature in turbulent combustion. PhD dissertation, 1992, Department of Mechanical Engineering, University of Leeds.